

This Page Is Inserted by IFW Operations
and is not a part of the Official Record

BEST AVAILABLE IMAGES

Defective images within this document are accurate representations of the original documents submitted by the applicant.

Defects in the images may include (but are not limited to):

- BLACK BORDERS
- TEXT CUT OFF AT TOP, BOTTOM OR SIDES
- FADED TEXT
- ILLEGIBLE TEXT
- SKEWED/SLANTED IMAGES
- COLORED PHOTOS
- BLACK OR VERY BLACK AND WHITE DARK PHOTOS
- GRAY SCALE DOCUMENTS

IMAGES ARE BEST AVAILABLE COPY.

**As rescanning documents *will not* correct images,
please do not report the images to the
Image Problem Mailbox.**

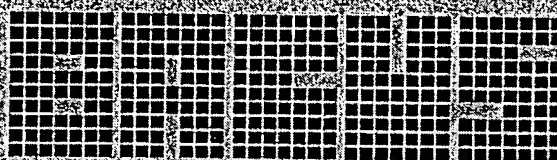
PROCEEDINGS OF SPIE

22nd Annual BACUS Symposium on Photomask Technology

Brian J. Grenon
Kurt R. Kimmel
Chairs/Editors

1-4 October 2002
Monterey, California, USA

Sponsored by



The international technical group of SPIE
dedicated to the advancement of photomask technology

SPIE - The International Society for Optical Engineering



Volume 4889
Part Two of Two Parts

- 1181 **Complementary double-exposure technique (CODE) solutions to the two-dimensional structures of 90-nm node [4889-135]**
S. Manakli, STMicroelectronics (France) and Lab. des Technologies et de la Microélectronique (France); Y. Trouiller, CEA-LETI (France); O. Toubian, Mentor Graphics Ltd. (France); P. Schiavone, Lab. des Technologies et de la Microélectronique (France); Y. F. Rody, Philips Research Labs. (France); P. J. Goirand, STMicroelectronics (France)
- 1189 **Application of chromeless phase lithography (CPL) masks in ArF lithography [4889-136]**
B. S. Kasproicz, C. J. Proglor, Photronics Inc. (USA); W. Wu, W. Conley, L. C. Litt, Motorola Inc. (USA); D. J. Van Den Broeke, K. E. Wampler, ASML Masktools Inc. (USA); R. J. Socha, ASML (USA)
- 1202 **PSM defect printability of extremely low-k1 sub-130-nm KrF lithography [4889-137]**
W.-I. Cho, G. Yeo, S.-Y. Moon, H.-S. Yoon, J.-M. Sohn, Samsung Electronics Co., Ltd. (South Korea)
- 1209 **Analytical approach to X-phenomenon in alternating phase-shifting masks [4889-138]**
J. R. Park, S.-H. Kim, H.-J. Lee, I.-Y. Jang, Y.-H. Choi, S.-H. Yang, J.-Y. Lee, Y.-H. Kim, S.-W. Choi, H.-S. Yoon, J.-M. Sohn, Samsung Electronics Co., Ltd. (South Korea)
- 1217 **Effects of alternating aperture PSM design on image imbalance for 65-nm technology [4889-140]**
A. Kroyan, H.-Y. Liu, Numerical Technologies, Inc. (USA)
- 1227 **Advanced 193 tri-tone EAPSM (9% to 18%) for 65-nm node [4889-141]**
L. Dieu, E. L. Fanucchi, G. P. Hughes, DuPont Photomasks, Inc. (USA); J. G. Mallabes, Motorola, Inc. (USA); D. L. Mellenthin, DuPont Photomasks, Inc. (USA); W. Conley, L. C. Litt, K. Lucas, Motorola, Inc. (USA); R. J. Socha, K. E. Wampler, A. Verhappen, J. Kluten, ASML (USA)
- 1234 **LithoScope: simulation-based mask layout verification with physical resist model [4889-142]**
Q.-D. Qian, IC Scope Co. (USA)
- 1242 **Imaging 100-nm contacts with high-transmission attenuated phase-shift masks [4889-143]**
J. V. Beach, International SEMATECH (USA); J. S. Petersen, Petersen Advanced Lithography, Inc. (USA); B. G. Eynon, D. Taylor, Photronics Inc. (USA); D. J. Gerold, M. J. Maslow, Petersen Advanced Lithography, Inc. (USA)
- 1253 **Validation of ArF chromeless PSM in the sub-100-nm node DRAM cell [4889-144]**
J.-H. Lee, D.-H. Chung, D.-C. Cha, H.-S. Kim, J.-S. Park, D.-G. Nam, S.-K. Woo, H.-S. Cho, W.-S. Han, Samsung Electronics Co., Ltd. (South Korea)
- 1263 **Alt-PSM of contact with phase-assist feature for 65-nm node [4889-145]**
J.-W. You, J.-J. Shin, C.-H. Chang, L.-W. Kung, B.-C. Chang, C.-M. Dai, T.-S. Gau, B. J. Lin, Taiwan Semiconductor Manufacturing Co., Ltd. (Taiwan)
- 1273 **Preliminary study of 65-nm-node alternating phase-shift mask fabrication [4889-146]**
K. Hosono, N. Ishiwata, S. Asai, H. Maruyama, Y. Miyahara, Fujitsu Ltd. (Japan); S. Sanki, Y. Yamashita, Y. Hotta, T. Furukawa, M. Naito, H. Miyashita, S. Noguchi, Dai Nippon Printing Co., Ltd. (Japan)
- 1281 **Model-based OPC using the MEEF matrix [4889-147]**
N. B. Cobb, Y. Granik, Mentor Graphics Corp. (USA)

Application of Chromeless Phase Lithography (CPL) masks in ArF lithography

Bryan S. Kasprovicz¹, Christopher J. Proglor¹, Wei Wu², Will Conley², Lloyd C. Litt²,
Doug Van Den Broeke³, Kurt E. Wampler³, Robert Socha⁴

¹Photronics, Inc.
601 Millennium Dr., Allen, TX 75013

²Motorola, Inc.
Advanced Optical Lithography Group
3501 Ed Bluestein Blvd., MS K10, Austin, TX 78721

³ASML MaskTools & ⁴ASML Technology Development Center
4800 Great America Parkway, Suite 400, Santa Clara, CA 95054

1. ABSTRACT

The challenges of low k_1 lithography require unique solutions at all levels of the lithography process. Chromeless phase lithography (CPL) is a promising technique that uses a 2-beam imaging strategy and a unique OPC application for enhanced CD uniformity through pitch. It is particularly effective when combined with a high numerical aperture (NA) and off-axis illumination (OAI). In addition to its imaging benefits, CPL masks offer many advantages in the manufacturing of the mask over other approaches.

The manufacturing strategy and methodology employed to fabricate CPL masks will be discussed. The technical challenges of mask production will also be highlighted. Application of CPL to production ArF images were characterized through simulations and experimental data demonstrating the capability of this technique to produce complex structures.

Keywords: PSM manufacturing, Chromeless Phase Lithography, CPL, PSM, high transmission attenuated PSM, chromeless mask

2. INTRODUCTION

Lithographers are continuously trying to improve process windows for a manufacturing technology and developing new options for the next technology node. An easy way to achieve improvements in resolution is simply to migrate to a shorter wavelength. Unfortunately, a change in wavelength typically requires a large capital expense and significant process development effort. Alternatively, off-axis illumination techniques such as annular and quadrupole can be applied to enhance an existing process. All high-end exposure systems in use have the ability to utilize several different illumination schemes, so alternate illumination implementation is relatively transparent to the lithographer unless one begins looking at custom apertures. As the cost of tools continues to rise combined with the uncertainty of the next technology, more focus is being placed on extending the current equipment capabilities.

Taking advantage of off-axis illumination (OAI) schemes will not achieve the desired results alone. Using OAI in combination with resolution enhancement techniques (RET) are also being pursued. Optical proximity correction (OPC) is currently in mainstream use and phase shift masks (PSM) are becoming more so.

Original manuscript in color: bkasprovicz@dallas.photronics.com, 972-889-6351

One of the solutions for increased exposure latitude and depth of focus enhancements is the alternating degree phase shift mask (AAPSM). Trenches are etched into the quartz mask substrate to generate a 180-degree phase shift relative to those areas of glass that were not etched. The resulting phase differences lead to interference, which results in higher contrast of the image. The inherent spatial frequency doubling of two-beam imaging results in an improvement in resolution as is illustrated in Figure 1. The most common type of AAPSM is known as complementary (CPSM). This type of solution utilizes a dual mask strategy. The first mask contains the phase-shifted geometry and the second is a binary mask that is used to remove unwanted phase edges caused by the initial exposure and has been discussed in detail by others.¹⁻⁵

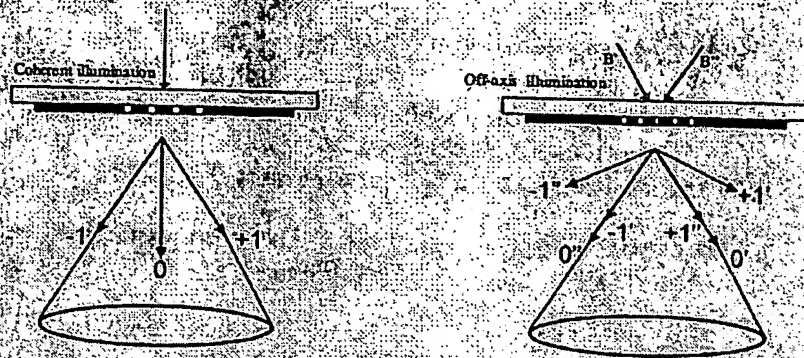


Figure 1. Comparison of three-beam versus two-beam imaging techniques.

A novel technique created by Chen et al. is the Chromeless Phase Lithography (CPL).⁶ This application of AAPSM can be thought of as a 100% attenuated PSM, using three-beam imaging, and can therefore be integrated with OAI. CPL offers many added benefits to the lithographer and mask maker in terms of performance, simplicity and cycle time. For the lithographer, the designs and verifications are simplified. There is no requirement for phase assignments, there are also no phase conflicts that require resolution as seen with AAPSM and the technology is less sensitive to phase errors. Since this is a single mask solution, there is no need for a second "cut mask" exposure thereby improving stepper throughput relative to an AAPSM implementation. As mask makers gained experience fabricating AAPSM's many of the challenges have been overcome. This work will highlight those challenges and present, for the first time — design, reticle and wafer data — from a CPL mask using 193nm lithography.

3. EXPERIMENTAL METHODS

3.1 The CPL mask process flow and characterization

There are several different design methodologies that can be considered when implementing CPL.⁷ Each will have its own unique process flow and set of challenges to overcome. For the purposes of this work, only the hybrid-mesa design was considered. Figure 2 shows an example of the incoming data and its transformation into a CPL design.

The basic process flow for the hybrid-mesa design is somewhat similar to that of the CPSM flow in that it requires two writes in order to achieve the 180-degree phase shift. A brief overview of the CPL process flow is shown in Figure 3. The initial patterning step defines the critical features, in this case the target was 300nm, and will be represented as a mesa in quartz or by an OPC structure in chrome. The subsequent pattern defines 0-degree areas and the critical chrome shielding structures that will prevent the strong optical proximity effects when pushing low k1 imaging.

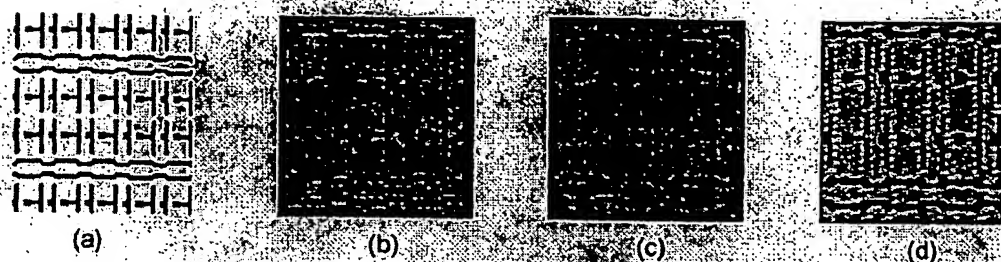


Figure 2. (a) Incoming design data, (b-d) outputted data after receiving phase assignments and OPC representing the 100nm, 75nm and 67nm nodes, respectively

Characterizations of the masks were performed using scanning probe metrology for depth and sidewall angles, scanning electron microscopy for CD's and inspected with an aggressive algorithm on a tool capable of handling the 65nm node.

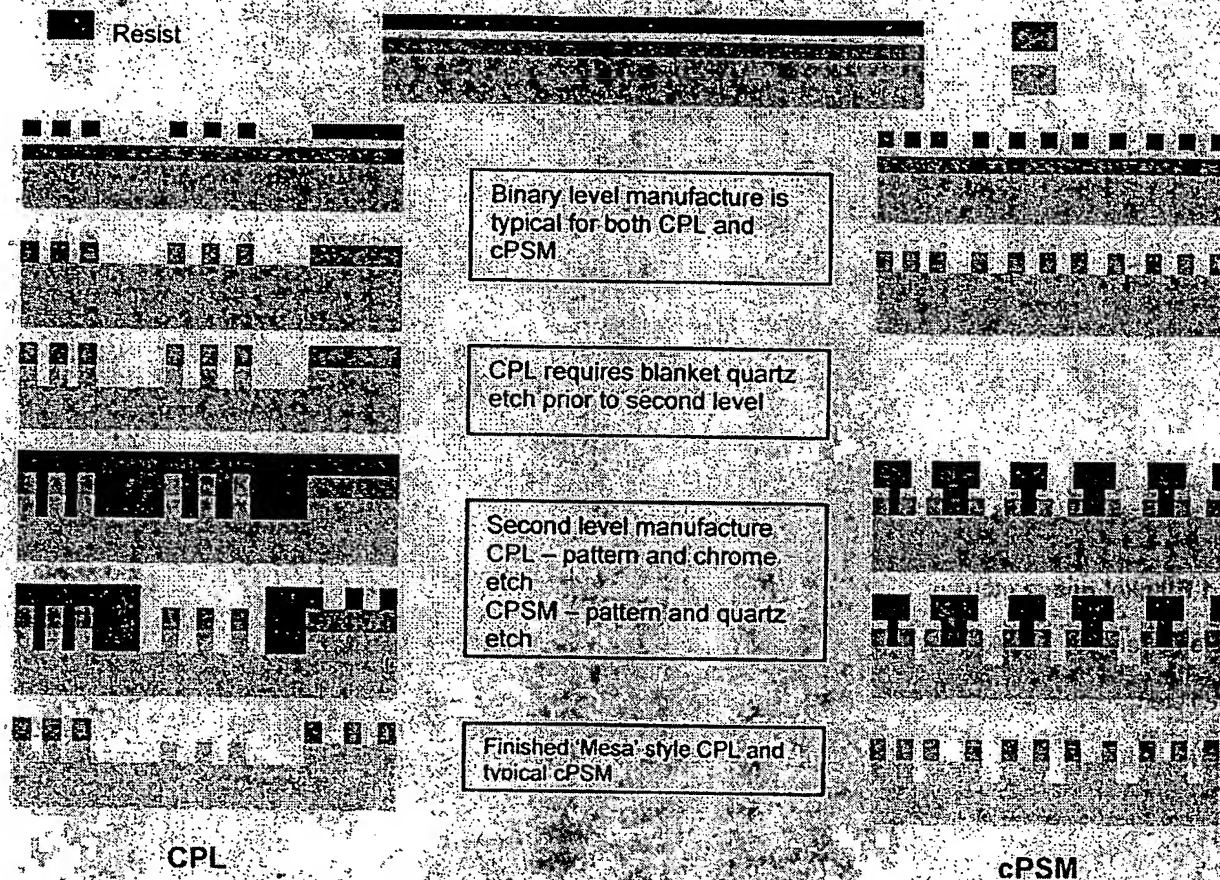


Figure 3. Typical reticle manufacturing flow and CPL as compared to cPSM.

3.2 Lithographic exposures and analysis

Test wafers were exposed through a range of focus and exposure conditions to determine the process capability. All of the exposures were performed on an ASML PAS 5500/1100 with several illumination conditions for different critical features. Resist thicknesses of 1600Å and 2200Å over an 800Å antireflective coatings were used for line-space and contact hole, respectively. A critical dimension of 0.100µm, 0.075µm and 0.067µm for line and space patterns along with 0.100µm for contacts was the target of this work. All simulations were conducted with Prolith version 7.2 and LithoCruiser Version 1.2 along with ProData version 1.3 for all ED window analysis.

4.0 RESULTS and DISCUSSION

Reticle Manufacture

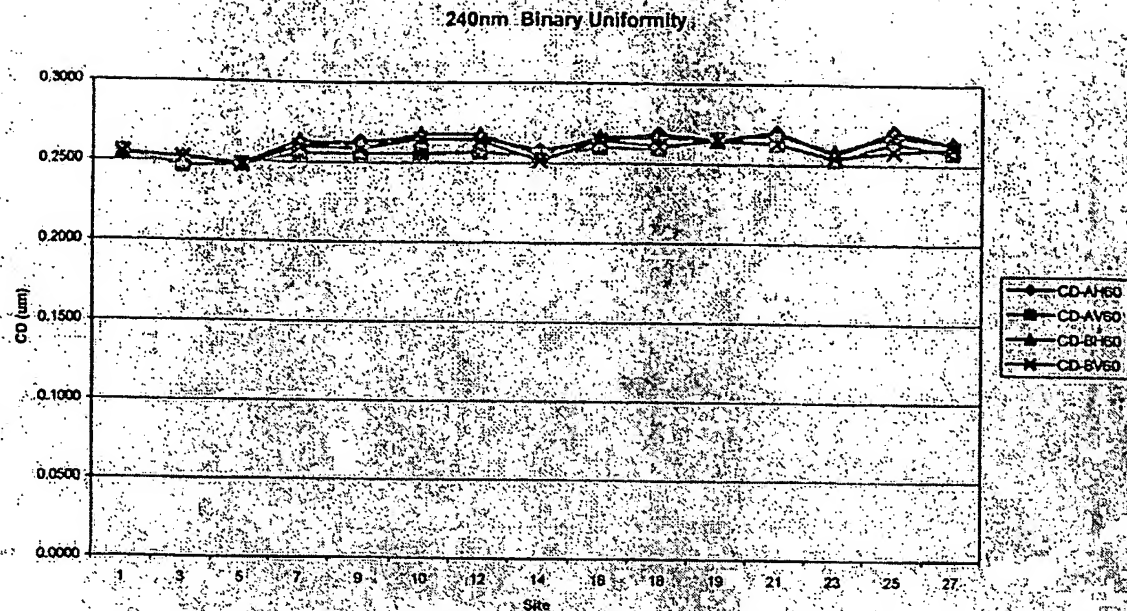
Chromeless phase lithography required development of a new process flow relative to cPSM. There were many considerations that were made to minimize the impact of the unknowns; however as the process in Figure 3 was being developed for the manufacture of the CPL reticles, several technical challenges were encountered and are identified in Table 1 below.

Impact to cPSM	Technical Challenge	Impact to CPL
Inspection	Blanket quartz etch	AR loss, depth uniformity, sidewall angle
Inspection strategy	AR coating loss or notching	Alignment, writer inspection
Overlay	Aggressive OPC	Inspection strategy
	Metrology – CD and depth	Accuracy, repeatability
	Second level write	CD targeting, overlay
Phase defects	Inspection	Phase defects

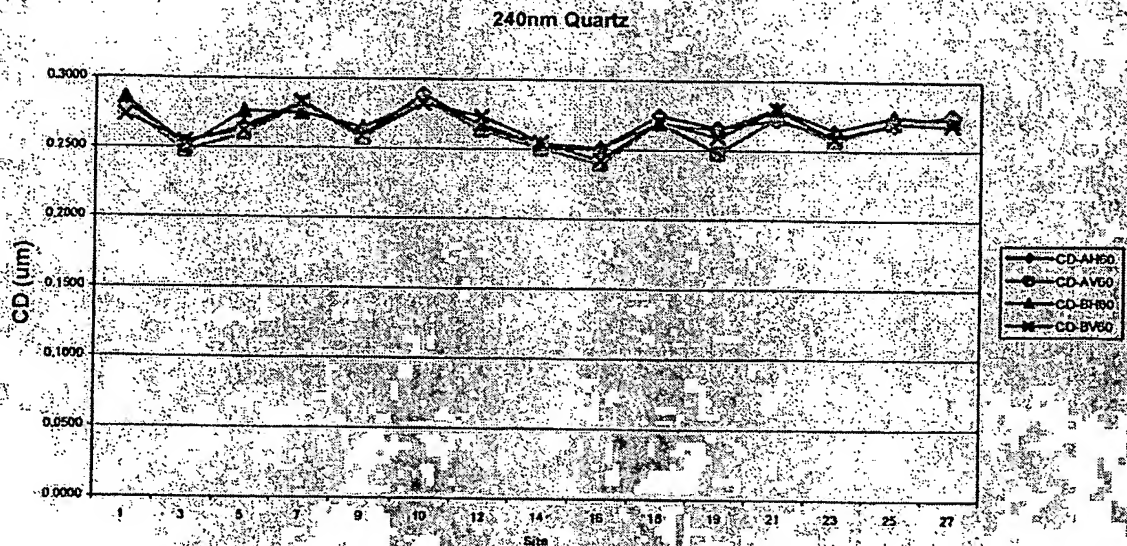
Table 1. Technical challenges to building cPSM and CPL phase-shift masks.

4.1 Blanket quartz etch with chrome as a hard mask

The current process flow requires a high-end binary level that is defect free prior to committing to the blanket quartz etch using chrome as a hard mask. Under the current process conditions the plasma is carbon depleted and any available oxygen readily accepts the carbon from the source chemistry. In doing so the passivation is out of balance and etch uniformity suffers, which can be stabilized by eliminating or adding different chemistry. Figure 4 (a-c) illustrates an example of carbon interaction on CD's pre (binary level) and post quartz etch.



(a)



(b)

Figure 4. (a) An example of the binary level CD uniformity prior to the blanket quartz etch and (b) CD uniformity after quartz etch.

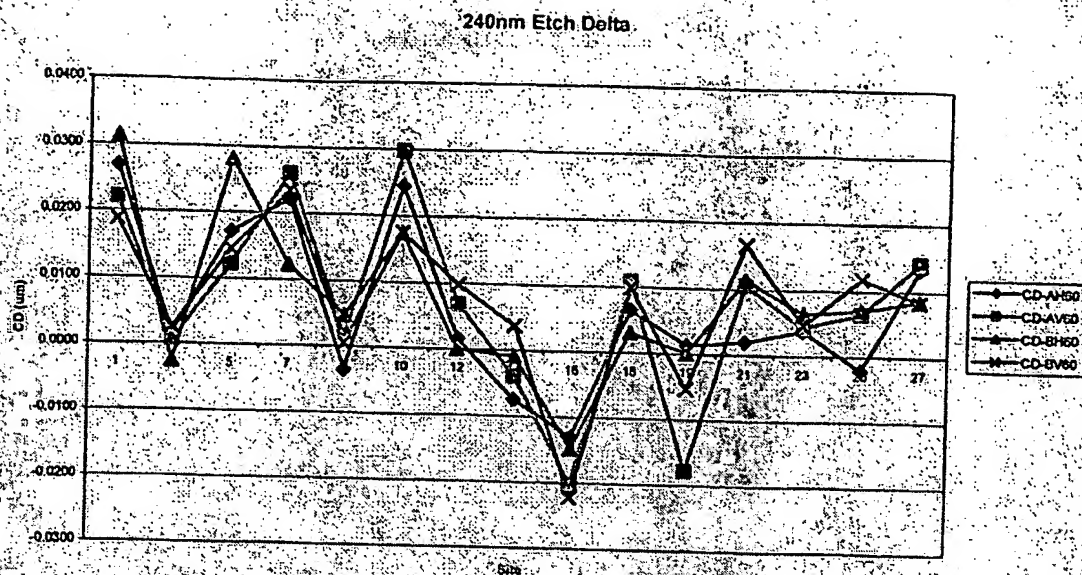


Figure 4c. CD delta between the binary level and etched quartz.

4.2 Antireflective coating loss

After completion of the binary level, the reticle is immediately subjected to a quartz etch. During this process the anti-reflective coating is removed, leaving the pure chrome exposed. This presents several challenges in other areas such as; inspection, depth metrology and second level processing that will be described in more detail later. As the anti-reflective coating begins to erode and approaches zero, the optical density remains above the standard 3.0 (transmission through the chrome of less than 0.10%), however there is a significant increase in the reflectivity from the top of the chrome at all wavelengths, both modeled in Figure 5 (a & b).

Although they have not yet been explored in detail, it is interesting to mention that this anti-reflective coating erosion (increased reflectivity) impacts multiple process steps in the reticle and wafer manufacturing lines. The typical inspection and second level reticle exposure tools use a ~365nm wavelength, the alignment laser is 532nm and the wafer exposure tool uses either 193nm or 248nm.

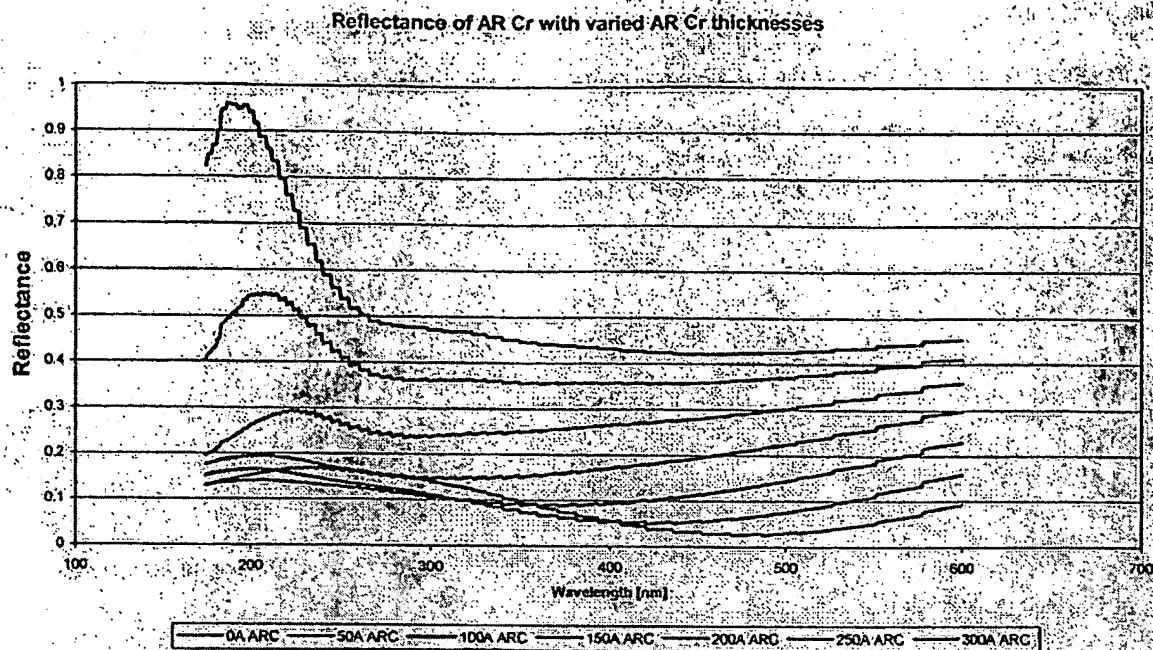


Figure 5a. Amount of reflectivity through critical wavelengths as the anti-reflective coating is removed.

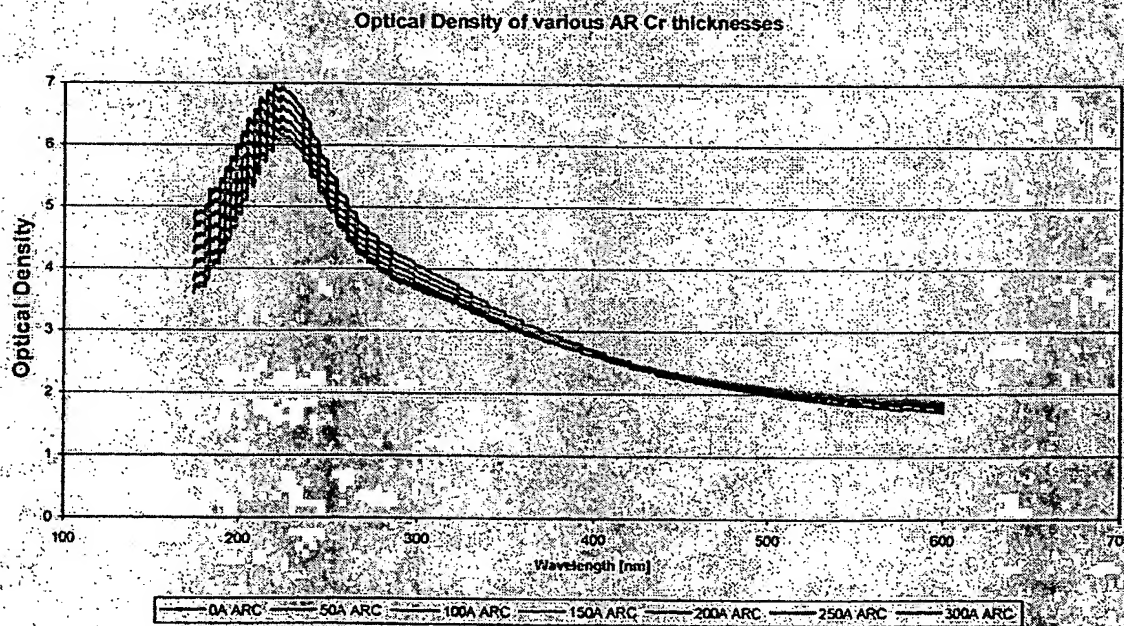


Figure 5b. Optical density through critical wavelengths as the anti-reflective coating is removed. Industry standard is 3.0, which is equivalent to a transmission of 0.10%.

4.3 Inspection Strategy

When considering low k1 imaging at 193nm, typical results for critical feature sizes are on the order of 250nm (4X) and OPC structures that approach 100nm. These feature sizes are not conducive to a robust inspection strategy, as the current state of the art inspection tools cannot process these features with high confidence.

As this is a hybrid-mesa design, the anti-reflective coating loss also presents itself as a problem for the inspection tools if the reflectivity varies significantly between the 0 degree and 180 degree areas. As shown in Figure 6 a tri-tone inspection problem will exist. Current inspection algorithms are not capable of addressing this technical challenge.

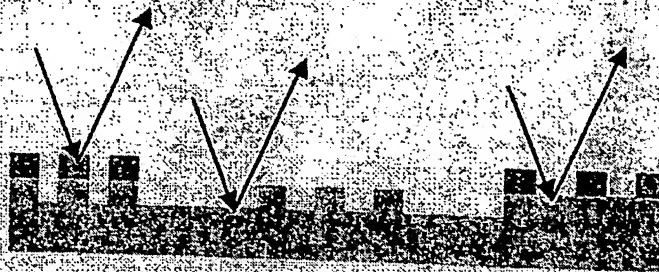


Figure 6. An example of the three different reflectivity's that may be realized from a CPL mask.

4.4 Accurate depth and CD measurements

The 180-degree phase is achieved by using a blanket fluorine etch over the entire plate delineates the quartz trenches. Hence the true depth is not known until after the second level chrome etch is complete thereby exposing the 0 degree portions for reference, shown in Figure 7. In addition, a typical standard chrome blank could have a chrome stack (includes chrome and antireflective coating) uniformity that is as much as 80Å across the entire reticle. If the reticle is to be measured prior to second level exposure, then this variation will impact the overall accuracy of the depth measurements. As the phase is a function to the refractive index and alone.

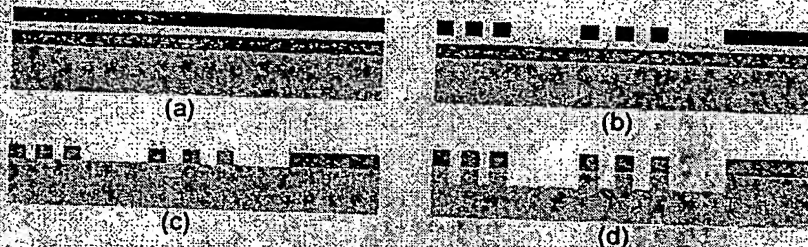


Figure 7. Reticle cross-sections from first level. (a) standard blank, (b) after processing, (c) after chrome etch and (d) after blanket quartz etch – sidewall angle is >90 degrees. The 0-degree regions are not defined until second level processing.

The sidewall angle of any type of feature, independent of material will influence the CD metrology precision from any tool. In this particular case, all CD's were measured using a SEM with a threshold of 50%, which is approximately the midpoint on the depth of the feature. As the sidewall changes between 80 to 85 degrees, there is a 4-5nm relative change in CD. A way to combat this effort is with surface probe metrology. This allows an opportunity to obtain the sidewall angle, depth and CD all in one comprehensive scan, however current tools do not offer the required repeatability or throughput to make them a viable solution to measure CD's.

4.5 Second level write

There are several concerns regarding the impact of the CPL manufacturing methodology on the second level write performance, namely the alignment capability due to increased reflectivity of the pure chrome versus the chrome/ARC stack having etched quartz features as the primary alignment marks plus the sensitivity of dose control as critical features are being defined.

Figure 4 highlights the impact of the missing AR at the nominal 532nm wavelength for the alignment laser on the write tool. The reflectivity at this wavelength increases by an order of magnitude and may end up helping the overall alignment detection capability by improving contrast between the chrome and quartz.

Having critical features during the second level write is rather unique to CPL when compared to other AAPSM techniques. Figure 8 shows an example of a cPSM and CPL second level writes. The critical feature size of a typical cPSM design representing the 75nm is on the order of 1 μ m, which is about twice the size of the critical feature of the CPL technology. As with all lithography processes this can be compensated through several techniques and should not pose a major challenge, however there are legitimate concerns. When adjusting this process to achieve the critical feature, the impact to the other challenges needs to be understood.



Figure 8. Typical second level writes for (a) CPL and (b) cPSM technologies.

Preliminary ArF exposures

4.6 Simulated and Experimental

Simulations to investigate the overlapping process window for 0.07 μ m through pitch were completed with Prolith version 7.2. The imaging conditions were 0.75NA with Quasar off axis illumination with an outer σ of 0.87 and an inner σ of 0.57. There were a number of pitches examined starting at 0.18 μ m to 0.50 μ m. The overlapping process windows for the 0.07 μ m through pitch imaging are plotted in Figure 9. The overlapping process window contains approximately 0.3 μ m DOF at 5% dose latitude.

In Figure 10 the image to the far left represents lithography for the 0.075 μ m SRAM with the corresponding mask design in the middle and mask build to the right. The middle picture in figure b is the actual layout with the phase depicted in blue with the field depicted in red and chrome is in black. The NA for these 193nm exposures was 0.75 with 0.87 to 0.57 using quasar illumination. Wafer imaging was completed in 0.21 μ m of resist over 0.082 μ m of a bottom antireflective coating.

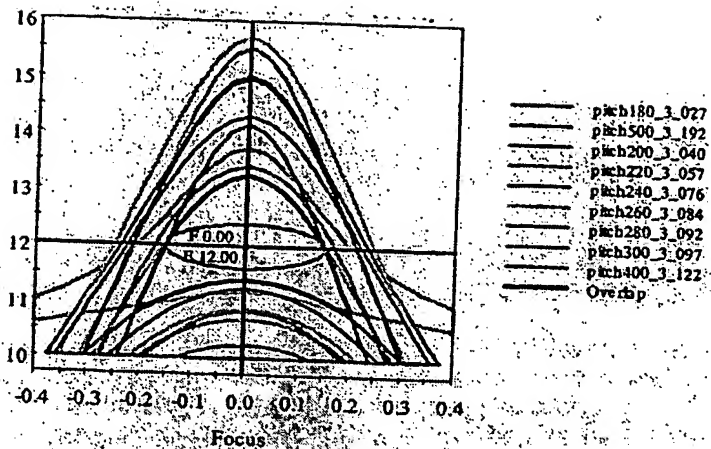


Figure 9. Overlapping imaging process windows for the 70nm feature through pitch

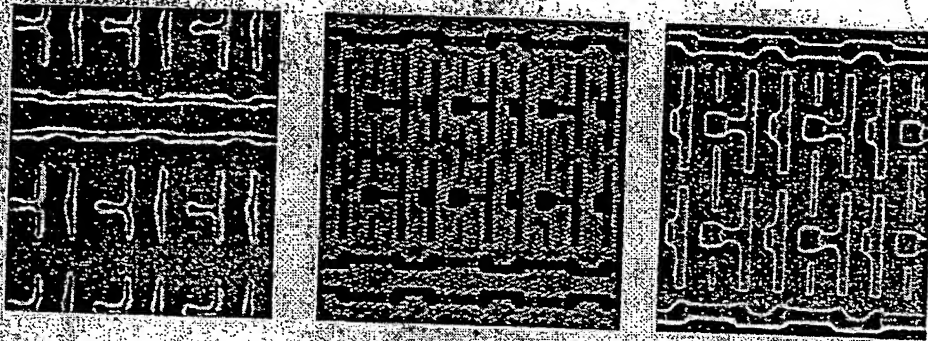


Figure 10. Examples of 75nm design, reticle and wafer results

Figure 11 is a Bossung plot for the above imaging SRAM gate structure. The critical dimension is $0.075\mu\text{m}$ demonstrating a good through dose and focus process. The authors have plotted an exposure-defocus window for the data shown in Figure 12. The exposure latitude is just over 30% at 0 focus & at $0.4\mu\text{m}$ defocus still remains a large dose window at 10%.

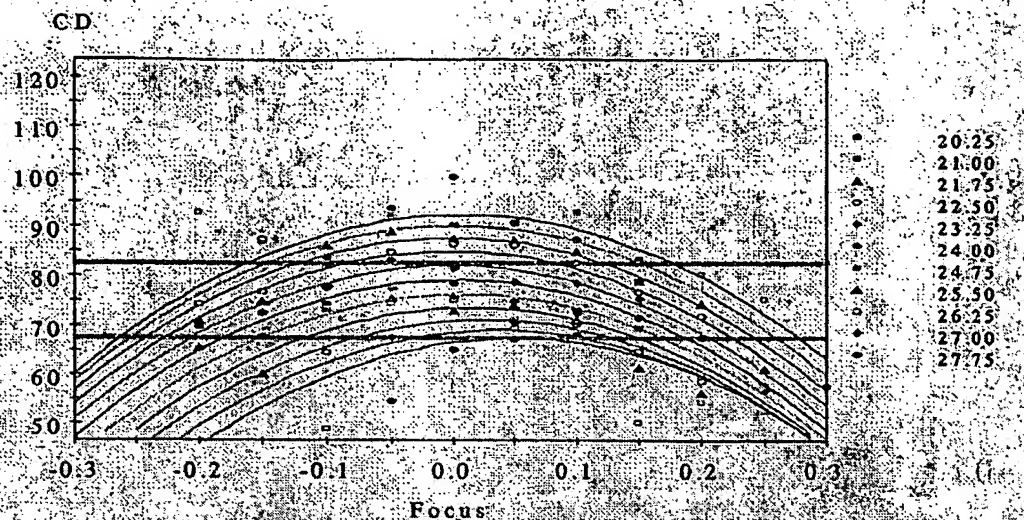


Figure 11. Bossung plot for 75nm SRAM gate structure

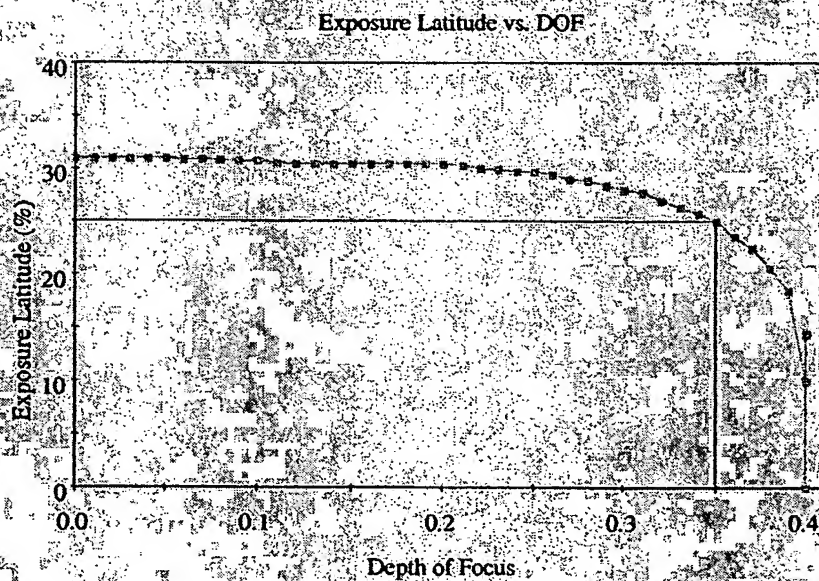


Figure 12. Exposure-defocus imaging window for 75nm SRAM gate structure.

In Figure 13 the authors have collected micrographs for the Bossung plot in Figure 11. The purpose is to confirm through the actual micrographs that the actual process window does exist.

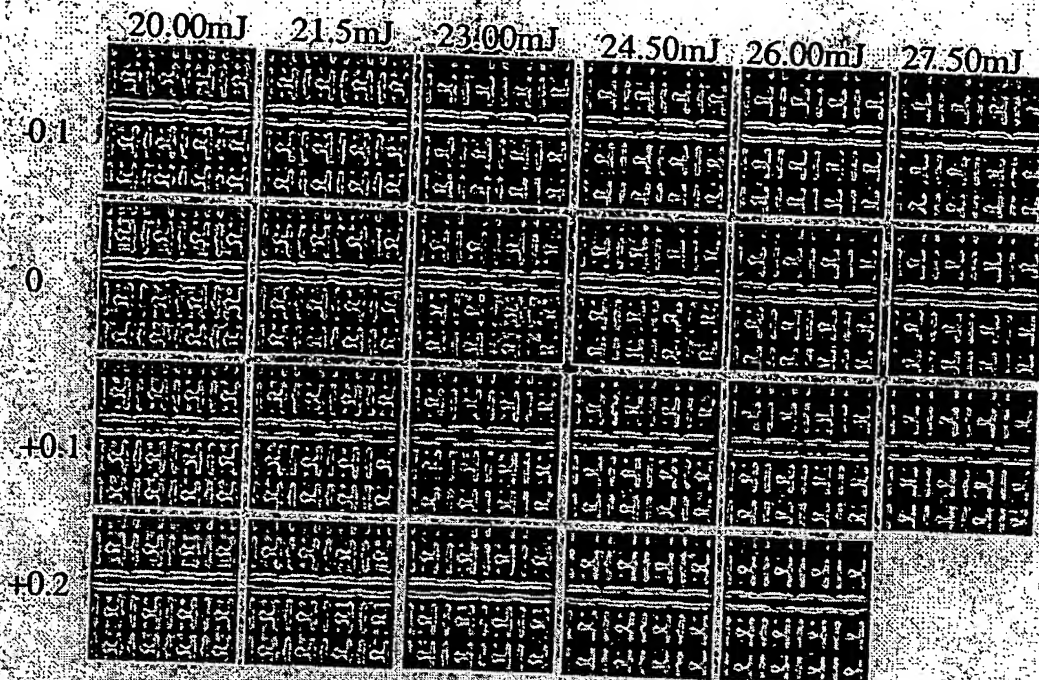


Figure 13. Micrographs of actual 75nm process window.

5.0 CONCLUSIONS

The new CPL technology brings with it a series of manufacturing challenges that will need to be addressed, however there are no showstoppers that would prevent it from becoming viable lithography solution for the future. Phase defect inspection remains a critical issue, as the current 'state of the art' inspection tool cannot process these features with high confidence.

6.0 FUTURE WORK

Optimization and tolerance of phase angle will need to be characterized in order to derive the CPL specification target and deviation of the quartz depth. Additional reticles were manufactured with a slightly different process flow to intentionally induce phase errors. The detectability and printability of chrome and phase defects will need to be evaluated as well.

7.0 ACKNOWLEDGEMENTS

The authors would like to thank Thomas Mathew, Eric Poortinga and Matt Lassiter of Photronics for their diligence in providing support during the reticle manufacture and for collecting the reticle characterization data. Robert Socha, Kurt Wampler, Fung Chen, Erika Schaefer, Shawn Cassel, and Linda Yu from ASML for their help with simulations, reticle design, wafer exposures and measurements.

8.0 REFERENCES

1. Wantanabe et al. "Sub-Quarter-Micron Gate Pattern Fabrication using a Transparent Phase Shift Mask", JVS Technology, B9(6), Nov/Dec 1991.
2. Toh et al., "Optical Lithography with Chromeless Phase-Shifted Masks", SPIE, vol. 1643, pp. 207-217, 1991.
3. Fritze et al. "Applications of Chromeless Phase-Shifting Masks to sub-100nm SOI CMOS Transistor Fabrication", SPIE, vol. 4000, pp. 388-407, 2000.
4. Patterson et al., "Effective Quartz Phase Etch on 193nm Alternating Phase Shift Mask Performance for the 100nm Node", SPIE, vol. 4691, pp. 1033-1040, 2002.
5. Karkin et al., "Automatic Defect Severity Scoring for 193nm Reticle Defect Inspection", SPIE, vol. 4346, pp. 898-906, 2001.
6. Chen et al., "System and Method of providing optical proximity correction for features using phase shifted halftone transparent/semi-transparent features", US Patent 6335130 B1.
7. Van Den Broeke et al., "Complex 2D Pattern Lithography at $\lambda/4$ Resolution Lithography using Chromeless Phase Lithography (CPL)", SPIE vol. 4691, pp. 196-214, 2002.